PAGEOPH, Vol. 148, Nos. 1/2 (1996) 0033-4553/96/020039-38$1.50 + 0.20/0

Accuracy of Elastic Finite Differences in Smooth Media

LUDĚK KLIMEŠ[1]

Abstract—The accuracy of finite-difference schemes of the 2nd and 4th order in 2-D and 3-D regular rectangular grids is studied. The method of designing the schemes and estimating their accuracy is proposed. The paper is devoted to the point schemes, expressed in terms of the discretized (point) values of the wave field and material parameters. Only the common schemes applicable in smooth parts of seismic models, outside structural interfaces, are taken into account. Finite differences at structural interfaces are studied elsewhere.

The inaccuracy of finite-difference schemes is governed, above all, by the error in the phase velocity, caused by discretization. This error is estimated for several finite-difference schemes. It is explicitly dependent on the direction of propagation and on wave polarization. The maximum phase-velocity error over all directions of propagation enables the accuracy of the individual schemes to be appreciated in order to select the best one. The proposed approach is general and applicable to other finite-difference schemes, for example, of the 6th and higher orders.

Key words: Seismic waves, finite differences of the 2nd and 4th order, 2-D and 3-D seismic modeling, accuracy, elasticity.

1. Introduction

The accuracy of finite-difference schemes of the 2nd and 4th order in 2-D and 3-D regular rectangular grids is studied in this paper. Only the point schemes, expressed in terms of the discretized (point) values of the wave field and material parameters, are considered. Since this paper is devoted to finite-difference calculation of *elastic waves*, the words *wave field* will stand for space-time dependent *displacement vector* throughout this paper.

Since the finite grid spacing causes the most severe problems at the highest frequencies contained within the wave forms, we concentrate especially on the high-frequency behavior of finite-difference schemes. From this point of view, the optimum finite-difference schemes built on a given small neighborhood of each point are the schemes designed by means of truncated Taylor expansions. We consider *centered* (sometimes also called *conventional*, e.g., by STEPHEN 1988) point

[1] Department of Geophysics, Charles University, Ke Karlovu 3, 121 16 Praha 2, Czech Republic.

finite-difference schemes of the 2nd and 4th order with all wave-field values and material parameters specified or calculated at the gridpoints, and *staggered* schemes of the 2nd and 4th order according to MADARIAGA (1976), VIRIEUX and MADARIAGA (1982), VIRIEUX (1986), LEVANDER (1988) and SEI (1993), with wave-field values calculated half way between gridpoints along the corresponding gridlines, the diagonal stress components evaluated at the gridpoints and the mixed stress components evaluated at the centers of the square faces formed by the corresponding gridlines.

In Sections 2 and 3, the method of designing the centered point finite-difference schemes applicable in smooth parts of seismic models, outside structural interfaces, is presented. The method is suitable both in isotropic and anisotropic seismic models. The schemes have a general form of linear operators acting on the wave-field grid values. These finite-difference schemes may be generalized for application in the vicinity of structural interfaces. The application at structural interfaces is presented elsewhere in order to keep this paper concise and readable.

In Sections 4 and 5, the tools for estimating the accuracy of finite-difference schemes are presented. The harmonic wave field is *locally* considered to be composed of P and S waves propagating with the corresponding *phase velocities*. The inaccuracy of finite-difference schemes is governed especially by the error in the phase velocity, caused by discretization. The presented methods for estimating the accuracy of finite-difference schemes are applicable both to isotropic and anisotropic seismic models.

Section 6 shows the accuracy and other properties of several particular finite-difference approximations of individual partial wave-field derivatives ("partial schemes"). This analysis follows the method of Sections 2 and 3. The wave-field finite differencing is, of course, independent of anisotropy.

In Section 7, the relative phase-velocity error due to the inaccurate second partial wave-field derivatives in isotropic models is estimated. This error is estimated for several finite-difference schemes of the 2nd and 4th order in 2-D and 3-D regular rectangular grids. It is explicitly dependent on the direction of propagation and on wave polarization. The maximum phase-velocity error over all directions of propagation enables the accuracy of individual schemes to be appreciated in order to find the best one. Section 7 follows from Sections 5 and 6.

In Section 8, the relative phase-velocity error due to the inaccurate first partial wave-field derivatives is estimated.

In Section 9, the relative phase-velocity error due to the inaccurate first partial derivatives of the material parameters is estimated.

In Section 10, the relative phase-velocity error of the staggered finite-difference schemes due to the inaccurate values of the material parameters is briefly discussed.

The proposed approach is general and applicable to other finite-difference schemes, for example, of the 6th and higher orders.

2. Wave Field on a Rectangular Grid

Expressions of this Section firstly are devoted to the centered finite-difference schemes, however they should also be applicable to other (e.g., staggered) point finite-difference schemes with only minor modifications.

2.1. Gridpoints and Discretization

At a fixed time, the wave field is represented by grid values $u_i(\mathbf{x})$, where the positional vector $\mathbf{x}$ takes the values (positions) of all gridpoints. In the computer memory, the gridpoints are, as a rule, indexed. The positional vector $\mathbf{x}$ is then represented by the corresponding integer index, and $u_i(\mathbf{x})$ by an array.

Denote by $\mathbf{h}_i$ the vectorial grid intervals. If the grid is regular and rectangular in Cartesian coordinates, and the grid intervals are of the same length h in all directions, we may choose

$$\mathbf{h}_1 = (h, 0, 0)^{\mathrm{T}}, \quad \mathbf{h}_2 = (0, h, 0)^{\mathrm{T}}, \quad \mathbf{h}_3 = (0, 0, h)^{\mathrm{T}}. \tag{1}$$

Gridpoints $\mathbf{y}$, from the vicinity of fixed gridpoint $\mathbf{x}$ situated inside the grid, may then be expressed as

$$\mathbf{y} = \mathbf{x} + n_1\mathbf{h}_1 + n_2\mathbf{h}_2 + n_3\mathbf{h}_3 = \mathbf{x} + n_i\mathbf{h}_i, \tag{2}$$

where n_1, n_2, and n_3 are small whole numbers (integers). For instance, $n_i = -1, 0, 1$ for 3-D finite differences of the second order, and $n_I = -1, 0, 1$, $n_3 = 0$ for 2-D finite differences of the second order. If the gridpoints are indexed, grid intervals $\mathbf{h}_1, \mathbf{h}_2, \mathbf{h}_3$ are represented by the corresponding shifts of the index.

2.2. Taylor Expansion

For fixed gridpoint $\mathbf{x}$ situated inside the grid, we put

$$u_{i(n_1, n_2, n_3)} = u_i(\mathbf{x} + n_1\mathbf{h}_1 + n_2\mathbf{h}_2 + n_3\mathbf{h}_3). \tag{3}$$

These grid values are the arguments of a linear finite-difference operator. Within a smooth geological block, the grid values may be approximated by a Taylor expansion from gridpoint $\mathbf{x}$.

Let us denote the value and partial derivatives of the wave field at $\mathbf{x}$ by

$$U_i = u_i(\mathbf{x}), \quad U_{ij} = u_{i,j}(\mathbf{x}) = \frac{\partial u_i}{\partial x_j}(\mathbf{x}), \quad U_{ijk} = u_{i,jk}(\mathbf{x}) = \frac{\partial^2 u_i}{\partial x_j\, \partial x_k}(\mathbf{x}),$$

$$U_{ijkl} = u_{i,jkl}(\mathbf{x}) = \frac{\partial^3 u_i}{\partial x_j\, \partial x_k\, \partial x_l}(\mathbf{x}), \quad U_{ijklm} = u_{i,jklm}(\mathbf{x}) = \frac{\partial^4 u_i}{\partial x_j\, \partial x_k\, \partial x_l\, \partial x_m}(\mathbf{x}), \ldots. \tag{4}$$

Grid values (3) may then be approximated by

$$u_{i(n_1,n_2,n_3)} = U_i + hU_{ij}n_j + \frac{h^2}{2}U_{ijk}n_jn_k + \frac{h^3}{6}U_{ijkl}n_jn_kn_l + \frac{h^4}{24}U_{ijklm}n_jn_kn_ln_m + \cdots. \tag{5}$$

For fixed **x**, grid values (3) are arranged into vector **u**, and partial derivatives (4) into vector **U**. This means that all considered combinations of the indices of $u_{n(n_1,n_2,n_3)}$ are ordered in some way (e.g., $_{1(-2,-2,-2)}$, $_{2(-2,-2,-2)}$, $_{3(-2,-2,-2)}$, $_{1(-1,-2,-2)}$, $\cdots$, $_{3(2,2,2)}$), and that each combination $_{n(n_1,n_2,n_3)}$ represents a single index in vector **u**. Equal derivatives (e.g., U_{112} and U_{121}) are summed to form a single element of **U** (e.g., $U_{1[12]} = U_{112} + U_{121}$, where index $[i,j]$ corresponds to all permutations of i and j). This means that the spatial wave-field derivatives are represented by components $U_{i[jk\cdots]}$. All considered combinations of the indices of $U_{i[jk\cdots]}$ are ordered in some way (e.g., $_1$, $_2$, $_3$, $_{1[1]}$, $_{2[1]}$, $\cdots$, $_{1[11]}$, $_{2[11]}$, $\ldots$), and each combination $_{i[j,k,\cdots]}$ represents a single index in vector **U**.

Taylor expansion (5) may than be expressed as the linear transformation

$$\mathbf{u} = \mathbf{TU}, \tag{6}$$

where the elements of Taylor-expansion matrix **T**, projecting U_i, $U_{i[j]}$, $U_{i[jk]}$, $U_{i[jkl]}$, $U_{i[jklm]}$, ... onto $u_{n(n_1,n_2,n_3)}$, are

$$\begin{aligned}
T_{n(n_1,n_2,n_3):i} &= \delta_{ni},\\
T_{n(n_1,n_2,n_3):i[j]} &= \delta_{ni}hn_j,\\
T_{n(n_1,n_2,n_3):i[jk]} &= \delta_{ni}\frac{h^2}{2}n_jn_k,\\
T_{n(n_1,n_2,n_3):i[jkl]} &= \delta_{ni}\frac{h^3}{6}n_jn_kn_l,\\
T_{n(n_1,n_2,n_3):i[jklm]} &= \delta_{ni}\frac{h^4}{24}n_jn_kn_ln_m, \ldots.
\end{aligned} \tag{7}$$

The combinations representing the first index and the second index of each element of **T** are separated by a colon.

2.3. Evaluation of the Second Time Derivatives of the Wave Field from the Elastodynamic Equations

Let us consider general linear stress-strain relations

$$\sigma_{ij} = c_{ijkl}u_{k,l}, \tag{8}$$

where c_{ijkl} are the elastic parameters (stiffnesses). In an isotropic medium,

$$c_{ijkl} = \delta_{ij}\delta_{kl}\lambda + \delta_{ik}\delta_{jl}\mu + \delta_{il}\delta_{jk}\mu \tag{9}$$

with

$$\lambda = \rho(v_P^2 - 2v_S^2), \quad \mu = \rho v_S^2. \tag{10}$$

The second partial time derivative of the wave field is given by the elastodynamic equation

$$u_i'' = \rho^{-1} \frac{\partial \sigma_{ij}}{\partial x_j} = \rho^{-1}(c_{ijkl} u_{k,lj} + c_{ijkl,j} u_{k,l}), \tag{11}$$

and specifically at $\mathbf{x}$

$$u_i''(\mathbf{x}) = \rho^{-1}(C_{ijkl} U_{klj} + C_{ijklj} U_{kl}), \tag{12}$$

where

$$C_{ijkl} = c_{ijkl}(\mathbf{x}), \quad C_{ijklm} = \frac{\partial c_{ijkl}}{\partial x_m}(\mathbf{x}) \tag{13}$$

are the values and partial derivatives of the elastic parameters at central point $\mathbf{x}$. In an isotropic medium,

$$C_{ijkl} U_{klj} = (\lambda + \mu) U_{kki} + \mu U_{ikk}, \tag{14}$$

$$C_{ijklj} = \delta_{kl} \frac{\partial \lambda}{\partial x_i}(\mathbf{x}) + \delta_{il} \frac{\partial \mu}{\partial x_k}(\mathbf{x}) + \delta_{ik} \frac{\partial \mu}{\partial x_l}(\mathbf{x}), \tag{15}$$

and

$$C_{ijklj} U_{kl} = \frac{\partial \lambda}{\partial x_i}(\mathbf{x}) U_{kk} + \frac{\partial \mu}{\partial x_k}(\mathbf{x})[U_{ik} + U_{ki}]. \tag{16}$$

Partial derivatives C_{ijklm} of the elastic parameters at $\mathbf{x}$ may be approximated using symmetrical differences

$$C_{ijklm} = \frac{1}{2h}[c_{ijkl}(\mathbf{x} + \mathbf{h}_m) - c_{ijkl}(\mathbf{x} - \mathbf{h}_m)] \tag{17}$$

of the second order if all points $\mathbf{x} - \mathbf{h}_m$, $\mathbf{x}$, $\mathbf{x} + \mathbf{h}_m$ are situated in the same geological block. In other words, if the points are not separated by a structural interface. At structural interfaces, partial derivatives C_{ijklm} should preferably be calculated by model-specification software instead of differencing.

Equation (12) expresses the linear dependence

$$\mathbf{t} = \mathbf{S}\mathbf{U} \tag{18}$$

of vector

$$\mathbf{t} = (u_1'', u_2'', u_3'')^{\mathrm{T}} \tag{19}$$

on the vector **U** of the partial derivatives. The only nonzero components of matrix **S** are

$$S_{n:i[j]} = \rho^{-1} C_{ijnkk}, \quad S_{n:i[jk]} = \rho^{-1}(C_{ijkn} + C_{ikjn})/2, \tag{20}$$

projecting $U_{i[j]}$ and $U_{i[jk]}$ onto u''_n, respectively. The combinations representing the first index and the second index of each element of **S** are separated by a colon.

3. *Finite-difference Schemes Inside Geological Blocks*

To determine the spatial finite-difference scheme for a fixed time, we select N wave-field values at the gridpoints within the vicinity of each central point **x**. These N values determine vector **u** of the wave-field grid values. Equation (6) then represents N linear equations for the partial wave-field derivatives arranged in vector **U**. We thus must select N nonzero partial derivatives and put all other components of **U** equal to zero. The partial wave-field derivatives up to the second order must not be annulled. The set of N nonzero components of **U** must be selected so that the resulting system (6) of N linear equations for N nonzero components of **U** is regular. Thus, in our approach, the finite-difference scheme will be fully determined by selecting the set of N grid wave-field values (arguments of the scheme) and the set of N nonzero partial wave-field derivatives.

If a reasonable subset **u** of grid values (3) and the corresponding reasonable subset **U** of partial derivatives (4) is chosen, Taylor-expansion matrix **T** may be inverted and equation (6) can be solved,

$$\mathbf{U} = \mathbf{T}^{-1}\mathbf{u}. \tag{21}$$

Particular grid values (3) contained within vector **u** and partial derivatives (4) contained within vector **U** leading to each partial finite-difference scheme considered are given in Section 6, see e.g., (49) and (50) for the partial finite-difference scheme of Section 6.1. Vectors **u** and **U** leading to each finite-difference scheme considered in Section 7 are composed of the components corresponding to all partial schemes of which the finite-difference scheme is assembled.

From (7) it is obvious that the inverse Taylor-expansion matrix $\mathbf{T}^{-1}$ depends only on the grid structure and on the selected size and structure of vectors **u** and **U**, i.e., on the choice of the finite-difference scheme. Moreover, for a regular grid, the inverse Taylor-expansion matrix $\mathbf{T}^{-1}$ is the same for all "inner" gridpoints **x**. The finite-difference schemes of "inner" gridpoints do not cross the grid boundaries or structural interfaces.

The finite-difference scheme inside a smooth geological block may now be expressed in the general matrix form of

$$\mathbf{t} = \mathbf{S}\mathbf{T}^{-1}\mathbf{u}. \tag{22}$$

4. Accuracy of Finite-difference Schemes — Basic Concepts

4.1. Errors

Error $\delta(Q)$ of quantity Q is understood hereinafter as the deviation of the approximate value Q from value $\bar{Q}$ corresponding to the exact solution of the relevant equations,

$$\delta(Q) = Q - \bar{Q}. \tag{23}$$

4.2. Asymptotic Approximation of Wave-field Derivatives

First we introduce the parameters describing grid spacing with respect to the wavelength,

$$\epsilon_0 = -i\frac{2\pi H}{T}, \quad \epsilon = i\frac{2\pi h}{\Lambda}, \tag{24}$$

where H is the time step, h is the grid interval in space, T is the period and Λ is the wavelength of a monochromatic wave. We also denote

$$\epsilon_i = \epsilon\vartheta_i, \tag{25}$$

where ϑ_i are the components of the unit vector normal to the wave front. The partial wave-field derivatives may then be roughly approximated at high frequencies by

$$u_i'' \simeq u_i\left(-i\frac{2\pi}{T}\right)^2 = u_i\left(\frac{\epsilon_0}{H}\right)^2 = u_i\left(\frac{v\epsilon}{h}\right)^2, \tag{26}$$

and

$$U_{ijk\cdots n} \simeq U_i\frac{\epsilon_j}{h}\frac{\epsilon_k}{h}\cdots\frac{\epsilon_n}{h}. \tag{27}$$

We have denoted by $u_i'' = \partial^2 u_i/\partial t^2$ the second partial wave-field derivative with respect to time.

4.3. Relative Phase-velocity Error

The error of the calculated wave field is caused by the inaccuracy of the evaluation of the second derivative u_i'' of the wave field with respect to time by means of the finite differences in space, and by the inaccuracy of the finite-difference scheme of the second order along the time axis.

Error $\delta(u_i'')$ in the second derivative u_i'' of the harmonic wave of a particular polarization has approximately the same effect on the wave propagation as a perturbation of the elastic parameters causing the perturbation

$$\delta(\Gamma_{ik}) = \frac{\delta(u_i'')u_k}{u_m'' u_m} \tag{28}$$

of the Christoffel matrix

$$\Gamma_{ik} \simeq \rho^{-1} C_{ijkl} \frac{\epsilon_j \epsilon_l}{v^2 \epsilon^2}. \tag{29}$$

Let us emphasize that the zero-order ray approximation is used here just to locally estimate the influence of small error $\delta(u_i'')$ in the second wave-field derivative on the wave propagation, not to approximate the calculated wave field. Equation (29) is thus only displayed for reader's convenience and is not used here.

The *principal component* of error $\delta(u_i'')$ in the second derivative u_i'' is the component along the polarization vector

$$e_i = U_i / \sqrt{U_m U_m}. \tag{30}$$

The principal component of error $\delta(u_i'')$ influences the corresponding eigenvalue of the Christoffel matrix and consequently the phase velocity. This error, $e_i \delta(u_i'')$, thus considerably influences the calculated wave field. Its real part generates the error in the phase velocity along the ray and, consequently, in travel time, whereas its imaginary part causes the errors in the amplitude of the calculated waves. Let us emphasize that the imaginary part of the principal component of the error in u_i'' causes the same corresponding relative deviation from the exact solution as does the real part of the same magnitude.

The *additional components* of error $\delta(u_i'')$ in the second derivative u_i'' are perpendicular to polarization vector e_i. They influence the eigenvectors of the Christoffel matrix but not its eigenvalues. The additional components of error $\delta(u_i'')$ in the second derivative u_i'' thus locally disturb the polarization of the wave field, but have no considerable influence on the phase velocity or on the magnitude of the wave-field amplitudes, as compared with the influence of the principal component of the error. As opposed to the principal component, the additional components of the error do not accumulate during wave propagation, with the exception of S waves in an isotropic medium, where the additional components of the error cause the frequency-dependent cumulative rotation of the polarization vectors. Although the final error in the vectorial amplitudes of S waves propagating in an isotropic medium due to the rotation may be of the same order as the error caused by the principal component of $\delta(u_i'')$, it is not taken into account in this paper. Thus, the additional components of error $\delta(u_i'')$ in the second derivative u_i'' are neglected here.

The error of $\delta(u_i'')$ in u_i'' causes the relative complex-valued error of

$$\Delta = \frac{1}{2} \frac{u_i \delta(u_i'')}{u_m u_m''} \tag{31}$$

in the phase velocity of the wave front along the ray. In view of (26), the above error may be approximated by

$$\Delta \simeq \frac{1}{2}\frac{H^2}{\epsilon_0^2}\frac{u_i\delta(u_i'')}{u_m u_m} = \frac{1}{2}\frac{h^2}{v^2\epsilon^2}\frac{u_i\delta(u_i'')}{u_m u_m}. \tag{32}$$

4.4. Distortion of Monochromatic Waves

The resulting relative error Δ_u (relative wave-form misfit) of the monochromatic wave field u_i, $\delta(u_i) \simeq u_i\Delta_u$, accumulated during time t along a ray of length s, is

$$\Delta_u \simeq -i\frac{2\pi}{T}\int_0^s \frac{\Delta}{v}\,\mathrm{d}s = -i\frac{2\pi}{T}\int_0^t \Delta\,\mathrm{d}t. \tag{33}$$

This error accumulates with increasing time of propagation and an instant of time occurs at which interference waves cannot be evaluated correctly (SEI, 1993). Thus, the relative phase-velocity error should be chosen inversely proportional to the time interval of the finite-difference calculation.

For example, if the average relative phase velocity error is 10^{-3}, the relative error of the calculated wave field (relative wave-form misfit) at time $t = 10\ T$ is about 6%, at time $t = 40\ T$ about 25%. If the average relative phase-velocity error is 10^{-2}, the relative error of the calculated wave field (relative wave-form misfit) at time $t = 8\ T$ is about 50%.

4.5. Distortion of Wave Packets

The relative phase-velocity error Δ increases with the Kth power of frequency $f = T^{-1}$, where K is the order of the finite difference scheme, $K = 2$ or $K = 4$. Then the wave fronts of the wave packet propagate along the ray with the relative velocity error of Δ approximately corresponding to the prevailing frequency, whereas the packet envelope propagates with the relative group-velocity error of

$$\Delta_G = \Delta + f\frac{\mathrm{d}\Delta}{\mathrm{d}f} = (K+1)\Delta. \tag{34}$$

Thus the erroneous time shift of the packet envelope, caused by the real part of the relative phase-velocity error, is $(K+1)$-times greater than the time shift of the wave fronts. This causes the phase shift of the wave packet of

$$-K\frac{2\pi}{T}\int_0^t \mathrm{Re}(\Delta)\,\mathrm{d}t. \tag{35}$$

Similarly, the relative amplitude error of the packet envelope, caused by the imaginary part of the relative phase-velocity error, is approximately $(K+1)$-times greater than the relative error of the amplitude of the monochromatic wave of the same prevailing frequency.

5. Sources of the Relative Phase-velocity Error

5.1. Error due to Finte Differences of the Second Order with Respect to Time

First, we shall study the error of the finite-difference scheme

$$u_i(\mathbf{x}, t+H) = 2u_i(\mathbf{x}, t) - u_i(\mathbf{x}, t-H) + H^2 u_i''(\mathbf{x}, t) \tag{36}$$

along the time axis.

The error of this scheme is produced by neglecting the fourth derivative u_i'''' with respect to time on the right-hand side. The error in u_i'' due to neglecting term $2(H^4/24)u_i''''$ is

$$\delta(u_i'') \simeq -\frac{H^2}{12} u_i'''' \simeq -\frac{H^2}{12} u_i \left(\frac{\epsilon_0}{H}\right)^4 = -\frac{H^{-2}}{12} u_i \epsilon_0^4. \tag{37}$$

Inserting this estimate into (32) we arrive at the relative phase-velocity error of

$$\Delta^{(0)} \simeq -\frac{1}{24}\epsilon_0^2 \tag{38}$$

corresponding to the second-order scheme (36), see equation (6) by DABLAIN (1986). For example, in choosing 40 time steps per one period, $H = T/40$, the relative phase velocity error is 10^{-3}, whereas for 13 time steps per one period, $H = T/13$, the relative phase velocity error is 10^{-2}. The relative group-velocity error is 3 times greater and, e.g., for $H = T/13$ the erroneous phase shift of wave packets at time $t = 13\,T$ is about $\pi/2$. However, this error may be eliminated by calculating fourth (or even higher) wave-field derivatives with respect to time by a recursive application of a spatial finite-difference scheme (IGEL *et al.*, 1995). This error may, to some extent, also be eliminated by means of time and phase corrections applied to the Gabor transforms of synthetic seismograms.

5.2. Error Due to Finite Differences in Space

The error of (12) is

$$\delta(u_i'') = \delta(\rho^{-1}C_{ijkl})U_{klj} + \rho^{-1}C_{ijkl}\delta(U_{klj}) + \rho^{-1}C_{ijklj}\delta(U_{kl}) + \delta(\rho^{-1}C_{ijklj})U_{kl}. \tag{39}$$

The values ρ^{-1} and C_{ijkl} of material parameters are assumed to be exact, $\delta(\rho^{-1}) = 0$ and $\delta(C_{ijkl}) = 0$, and the wave-field derivatives may be approximated by (27). Then

$$\delta(u_i'') = \rho^{-1}C_{ijkl}\delta(U_{klj}) + \rho^{-1}C_{ijklj}\delta(U_{kl}) + \rho^{-1}\delta(C_{ijklj})U_k\epsilon_l h^{-1}. \tag{40}$$

Inserting this into (32), we arrive at

$$\Delta - \Delta^{(0)} \simeq \frac{1}{2}\frac{1}{\rho v^2 \epsilon^2}\frac{U_i}{U_m U_m}[C_{ijkl}\delta(U_{klj})h^2 + C_{ijklj}\delta(U_{kl})h^2 + \delta(C_{ijklj})U_k\epsilon_l h]. \quad (41)$$

Assuming that the errors $\delta(U_{ij})$ and $\delta(U_{ijk})$ of the first and second wave-field derivatives may be expressed in terms of the corresponding relative errors Δ_j and Δ_{jk} of the finite-difference scheme,

$$\delta(U_{ij}) = U_{ij}\Delta_j \simeq U_i\epsilon_j h^{-1}\Delta_j, \quad (42)$$

$$\delta(U_{ijk}) = U_{ijk}\Delta_{jk} \simeq U_i\epsilon_j\epsilon_k h^{-2}\Delta_{jk}, \quad (43)$$

where no summation is taken over indices j and k, we arrive at

$$\Delta - \Delta^{(0)} \simeq \frac{1}{2}\frac{1}{\rho v^2 \epsilon^2}\frac{U_i}{U_m U_m} \times \left[\sum_{l=1}^{3}\sum_{j=1}^{3} C_{ijkl}U_k\epsilon_l\epsilon_j\Delta_{lj} + \sum_{l=1}^{3} C_{ijklj}U_k\epsilon_l h\Delta_l + \delta(C_{ijklj})U_k\epsilon_l h\right]. \quad (44)$$

The total relative phase-velocity error may then be expressed in the form of

$$\Delta = \Delta^{(0)} + \Delta^{(1)} + \Delta^{(2)} + \Delta^{(3)} + \Delta^{(4)}, \quad (45)$$

with

$$\Delta^{(1)} \simeq \frac{1}{2}\frac{1}{\rho v^2 \epsilon^2} e_i e_k \sum_{l=1}^{3}\sum_{j=1}^{3} C_{ijkl}\epsilon_l\epsilon_j\Delta_{lj} \quad (46)$$

being the relative phase-velocity error caused by the inaccurate second partial wave-field derivatives,

$$\Delta^{(2)} \simeq \frac{1}{2}\frac{h}{\rho v^2 \epsilon^2} e_i e_k \sum_{l=1}^{3} C_{ijklj}\epsilon_l\Delta_l \quad (47)$$

being the relative phase-velocity error caused by the inaccurate first partial wave-field derivatives, and

$$\Delta^{(3)} \simeq \frac{1}{2}\frac{h}{\rho v^2 \epsilon^2} e_i e_k \delta(C_{ijklj})\epsilon_l \quad (48)$$

being the relative phase-velocity error caused by the inaccurate first partial derivatives of the elastic parameters. Error $\Delta^{(4)}$ caused by the inaccurate values of the elastic parameters due to the interpolation between gridpoints applies especially to the staggered grids and is zero for the centered point finite-difference schemes, $\Delta^{(4)} = 0$.

These contributions $\Delta^{(1)}$, $\Delta^{(2)}$, $\Delta^{(3)}$ and $\Delta^{(4)}$ (if applicable) to the entire relative phase-velocity error Δ will be estimated in the following sections.

6. Partial Finite-difference Schemes

As mentioned above, the only partial wave-field derivatives at $\mathbf{x}$, appearing in equation (12) and thus influencing the time development of the wave field, are the first and second derivatives $U_{i[j]}$ and $U_{i[jk]}$.

Thus, we shall first study the relative errors Δ_j of $U_{i[j]}$, and Δ_{jk} of $U_{i[jk]}$, in approximation (21). Since the approximations of the individual partial derivatives in (21) are, to some extent, independent for most symmetric finite-difference schemes, we may decompose the finite-difference schemes into several partial schemes for individual partial derivatives, and to estimate the relative error of each partial derivative independently. These results will then be used to estimate the relative phase-velocity errors of the waves of particular polarizations (P, S_1 and S_2) in several finite-difference schemes.

The centered finite-difference schemes with all wave-field values and material parameters specified or calculated at the gridpoints, are composed of finite-difference schemes centered at gridpoints. On the other hand, the staggered schemes are, as a rule, composed of 1-D half-interval partial finite-difference schemes for the first partial derivatives.

For 1-D partial finite-difference schemes of even orders from 2 to 10 centered at gridpoints and for their accuracy refer, e.g., to BICKLEY (1941). For 1-D half-interval partial finite-difference schemes of even orders from 2 to 10 refer, e.g., to KELLER and PEREYRA (1978). For a general algorithm to generate arbitrary 1-D partial finite-difference schemes refer to FORNBERG (1988). For the 2-D partial finite-difference scheme of the 2nd order centered at a gridpoint refer, e.g., to ABRAMOWITZ and STEGUN (1964).

6.1. Partial Scheme, 1-D, 3-point, 2nd Order (Fig. 1)

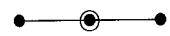

Figure 1

Wave-field grid values (arguments):

$$u_{i(n_1,0,0)}, \quad n_1 = -1, 0, +1. \tag{49}$$

Determined Taylor-expansion coefficients:

$$U_i, U_{i[1]}, U_{i[11]}. \tag{50}$$

Most important neglected Taylor-expansion coefficients:

$$U_{i[111]}, U_{i[1111]}. \tag{51}$$

Finite-difference equation for the first partial derivative inside a geological block (*1 floating-point operation* per $2hU_{i[1]}$):

$$2hU_{i[1]} = u_{i(+1,0,0)} - u_{i(-1,0,0)}. \tag{52}$$

Finite-difference equation for the second partial derivative inside a geological block (*3 floating-point operations* per $h^2U_{i[11]}$):

$$h^2U_{i[11]} = u_{i(+1,0,0)} + u_{i(-1,0,0)} - 2u_{i(0,0,0)}. \tag{53}$$

Relative error in $hU_{i[1]} \simeq U_i\epsilon_1$ due to neglecting $h^3U_{i[111]} \simeq U_i\epsilon_1^3$ inside geological blocks:

$$\Delta_1 = \frac{1}{2}\frac{1}{\epsilon_1}[1+1]\frac{\epsilon_1^3}{6} = \frac{1}{6}\epsilon_1^2. \tag{54}$$

Relative error in $h^2U_{i[11]} \simeq U_i\epsilon_1^2$ due to neglecting $h^4U_{i[1111]} \simeq U_i\epsilon_1^4$ inside geological blocks:

$$\Delta_{11} = \frac{1}{\epsilon_1^2}[1+1]\frac{\epsilon_1^4}{24} = \frac{1}{12}\epsilon_1^2. \tag{55}$$

Analogously in the directions of the 2nd and 3rd coordinate axes,

$$\Delta_j = \frac{1}{6}\epsilon_j^2, \tag{56}$$

$$\Delta_{j=k} = \frac{1}{12}\epsilon_j^2. \tag{57}$$

Note that the replacement of the homogeneous second partial difference (53) by double application of the first partial difference (52) produces 4 times increased relative error $\Delta_{j=k}$. This is the case of the conventional methods based on the first-order systems of equations for u_i and stress σ_{ij}.

6.2. Partial Scheme, 1-D, 5-point, 4th Order (Fig. 2)

Figure 2

Wave-field grid values (arguments):

$$u_{i(n_1,0,0)}, \quad n_1 = -2, -1, 0, +1, +2. \tag{58}$$

Determined Taylor-expansion coefficients:

$$U_i, U_{i[1]}, U_{i[11]}, U_{i[111]}, U_{i[1111]}. \tag{59}$$

Most important neglected Taylor-expansion coefficients:

$$U_{i[11111]}, \quad U_{i[111111]}. \tag{60}$$

Finite-difference equation for the first partial derivative inside a geological block (*4 floating-point operations* per $12hU_{i[1]}$):

$$12hU_{i[1]} = 8(u_{i(+1,0,0)} - u_{i(-1,0,0)}) - (u_{i(+2,0,0)} - u_{i(-2,0,0)}). \tag{61}$$

Finte-difference equation for the second partial derivative inside a geological block (*6 floating-point operations* per $12h^2U_{i[11]}$):

$$12h^2U_{i[11]} = 16(u_{i(+1,0,0)} + u_{i(-1,0,0)}) - (u_{i(+2,0,0)} + u_{i(-2,0,0)}) - 30u_{i(0,0,0)}. \tag{62}$$

Relative error in $hU_{i[1]} \simeq U_i\epsilon_1$ due to neglecting $h^5U_{i[11111]} \simeq U_i\epsilon_1^5$ inside geological blocks:

$$\Delta_1 = \frac{1}{12}\frac{1}{\epsilon_1}[8(1+1)-(32+32)]\frac{\epsilon_1^5}{120} = -\frac{1}{30}\epsilon_1^4. \tag{63}$$

Relative error in $h^2U_{i[11]} \simeq U_i\epsilon_1^2$ due to neglecting $h^6U_{i[111111]} \simeq U_i\epsilon_1^6$ inside geological blocks:

$$\Delta_{11} = \frac{1}{12}\frac{1}{\epsilon_1^2}[16(1+1)-(64+64)]\frac{\epsilon_1^6}{720} = -\frac{1}{90}\epsilon_1^4. \tag{64}$$

Analogously in the directions of the 2nd and 3rd coordinate axes,

$$\Delta_j = -\frac{1}{30}\epsilon_j^4, \tag{65}$$

$$\Delta_{j=k} = -\frac{1}{90}\epsilon_j^4. \tag{66}$$

Note that the replacement of the homogeneous second partial difference (62) by double application of the first partial difference (61) produces 6 times increased relative error $\Delta_{j=k}$. This is the case of the conventional methods based on the first-order systems of equations for u_i and stress σ_{ij}.

6.3. Partial Scheme, 2-D, 4-point, 2nd Order (Fig. 3)

This scheme for the mixed second derivatives is equivalent to the double application of the partial 1-D 3-point scheme (52) for the first derivatives.

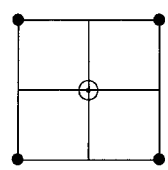

Figure 3

Wave-field grid values (arguments):

$$u_{i(\pm 1,\pm 1,0)}. \tag{67}$$

Determined Taylor-expansion coefficients in addition to 1-D partial schemes:

$$U_{i[12]},\ U_{i[112]},\ U_{i[122]},\ U_{i[1122]}. \tag{68}$$

Most important neglected Taylor-expansion coefficients in addition to 1-D partial schemes:

$$U_{i[1112]},\ U_{i[1222]},\ U_{i[11112]},\ U_{i[11122]},\ U_{i[11222]},\ U_{i[12222]}. \tag{69}$$

Finite-difference equation for the second partial derivative inside a geological block:

$$4h^2U_{i12} = 2h^2U_{i[12]} = u_{i(+1,+1,0)} - u_{i(-1,+1,0)} - u_{i(+1,-1,0)} + u_{i(-1,-1,0)}. \tag{70}$$

This could take 3 floating-point operations per $4h^2U_{i12}$. However, if the first derivatives resulting from (52) are stored, the evaluation of (70) by means of the second application of (52) takes only *1 additional floating-point operation* per $4h^2U_{i12}$.

Relative error in $h^2U_{i[12]} \simeq 2U_i\epsilon_1\epsilon_2$ due to neglecting $h^4U_{i[1112]} \simeq 4U_i\epsilon_1^3\epsilon_2$ and $h^4U_{i[1222]} \simeq 4U_i\epsilon_1\epsilon_2^3$ inside geological blocks:

$$\Delta_{12} = \frac{1}{2}\frac{1}{2\epsilon_1\epsilon_2}[1+1+1+1]\left(\frac{4\epsilon_1^3\epsilon_2}{24} + \frac{4\epsilon_1\epsilon_2^3}{24}\right) = \frac{1}{6}(\epsilon_1^2 + \epsilon_2^2). \tag{71}$$

Analogously in the x_1x_3 and x_2x_3 planes,

$$\Delta_{j\neq k} = \frac{1}{6}(\epsilon_j^2 + \epsilon_k^2), \tag{72}$$

which, of course, corresponds to errors (56) of the double application of (52) in directions j and k.

6.4. Partial Scheme, 2-D, 8-point, 4th Order (Fig. 4)

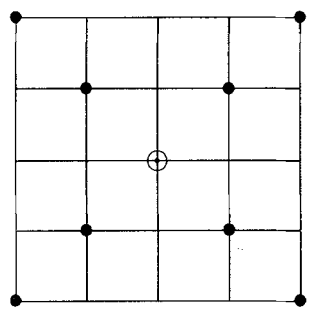

Figure 4

Wave-field grid values (arguments):

$$u_{i(\pm 1,\pm 1,0)}, \quad u_{i(\pm 2,\pm 2,0)}. \tag{73}$$

Determined Taylor-expasion coefficients in addition to 1-D 5-point partial schemes:

$$\begin{gathered} U_{i[12]},\ U_{i[112]},\ U_{i[122]},\ U_{i[1122]},\ U_{i[1112]} + U_{i[1222]}, \\ U_{i[11112]} + U_{i[11222]},\ U_{i[11122]} + U_{i[12222]}, \\ U_{i[111111]} + U_{i[111122]} + U_{i[112222]} + U_{i[222222]}. \end{gathered} \tag{74}$$

Most important neglected Taylor-expansion coefficients in addition to 1-D 5-point partial schemes:

$$\begin{gathered} U_{i[1112]} - U_{i[1222]},\ U_{i[11112]} - U_{i[11222]},\ U_{i[11122]} - U_{i[12222]}, \\ U_{i[111111]} - U_{i[111122]},\ U_{i[111111]} - U_{i[112222]},\ U_{i[111111]} - U_{i[222222]}, \\ U_{i[111112]},\ U_{i[111222]},\ U_{i[122222]}. \end{gathered} \tag{75}$$

Finite-difference equation for the second partial derivative inside a geological block (*8 floating-point operations* per $48h^2U_{i12}$):

$$\begin{aligned} 48h^2U_{i12} = 24h^2U_{i[12]} &= 16(u_{i(+1,+1,0)} - u_{i(-1,+1,0)} - u_{i(+1,-1,0)} + u_{i(-1,-1,0)}) \\ &\quad - (u_{i(+2,+2,0)} - u_{i(-2,+2,0)} - u_{i(+2,-2,0)} + u_{i(-2,-2,0)}). \end{aligned} \tag{76}$$

Relative error in $h^2U_{i[12]} \simeq 2U_i\epsilon_1\epsilon_2$ due to neglecting $h^6U_{i[111112]} \simeq 6U_i\epsilon_1^5\epsilon_2$, $h^6U_{i[111222]} \simeq 20U_i\epsilon_1^3\epsilon_2^3$, and $h^6U_{i[122222]} \simeq 6U_i\epsilon_1\epsilon_2^5$ inside geological blocks:

$$\begin{aligned} \Delta_{12} &= \frac{1}{24}\frac{1}{2\epsilon_1\epsilon_2}[16(1+1+1+1) - (64+64+64+64)]\left(\frac{6\epsilon_1^5\epsilon_2^1}{720} + \frac{20\epsilon_1^3\epsilon_2^3}{720} + \frac{6\epsilon_1\epsilon_2^5}{720}\right) \\ &= -\frac{1}{180}(6\epsilon_1^4 + 20\epsilon_1^2\epsilon_2^2 + 6\epsilon_2^4). \end{aligned} \tag{77}$$

Analogously in the x_1x_3 and x_2x_3 planes,

$$\Delta_{j\neq k} = -\frac{1}{180}(6\epsilon_j^4 + 20\epsilon_j^2\epsilon_k^2 + 6\epsilon_k^4). \tag{78}$$

6.5. Partial Scheme, 2-D, 12-point, 4th Order (Fig. 5)

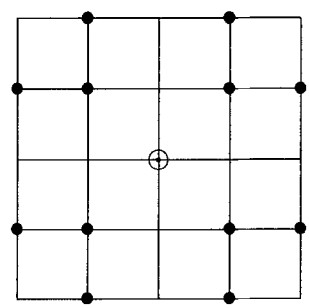

Figure 5

Wave-field grid values (arguments):

$$u_{i(\pm 1,\pm 1,0)},\ u_{i(\pm 2,\pm 1,0)},\ u_{i(\pm 1,\pm 2,0)}. \tag{79}$$

Determined Taylor-expansion coefficients in addition to 1-D 5-point partial schemes:

$$\begin{gathered} U_{i[12]},\ U_{i[112]},\ U_{i[122]},\ U_{i[1112]},\ U_{i[1122]},\ U_{i[1222]}, \\ U_{i[11112]},\ U_{i[11122]},\ U_{i[11222]},\ U_{i[12222]},\ U_{i[111122]},\ U_{i[112222]}. \end{gathered} \tag{80}$$

Most important neglected Taylor-expansion coefficients in addition to 1-D 5-point partial schemes:

$$\begin{gathered} U_{i[111112]},\ U_{i[111222]},\ U_{i[122222]}, \\ U_{i[1111112]},\ U_{i[1111122]},\ U_{i[1111222]},\ U_{i[1112222]},\ U_{i[1122222]},\ U_{i[1222222]}. \end{gathered} \tag{81}$$

Finite-difference equation for the second partial derivative inside a geological block (*12 floating-point operations* per $24h^2U_{i12}$):

$$\begin{aligned} 24h^2U_{i12} = 12h^2U_{i[12]} = 10(&u_{i(+1,+1,0)} - u_{i(-1,+1,0)} - u_{i(+1,-1,0)} + u_{i(-1,-1,0)}) \\ &- (u_{i(+2,+1,0)} - u_{i(-2,+1,0)} - u_{i(+2,-1,0)} + u_{i(-2,-1,0)}) \\ &- (u_{i(+1,+2,0)} - u_{i(-1,+2,0)} - u_{i(+1,-2,0)} + u_{i(-1,-2,0)}). \end{aligned} \tag{82}$$

Relative error in $h^2U_{i[12]} \simeq 2U_i\epsilon_1\epsilon_2$ due to neglecting $h^6U_{i[111112]} \simeq 6U_i\epsilon_1^5\epsilon_2$, $h^6U_{i[111222]} \simeq 20U_i\epsilon_1^3\epsilon_2^3$, and $h^6U_{i[122222]} \simeq 6U_i\epsilon_1\epsilon_2^5$ inside geological blocks:

$$\begin{aligned} \Delta_{12} = \frac{1}{12}\frac{1}{2\epsilon_1\epsilon_2}\Bigg[&(10\times 4 - 4\times 32 - 4\times 2)\times\frac{6\epsilon_1^5\epsilon_2}{720} \\ &+ (10\times 4 - 4\times 8 - 4\times 8)\times\frac{20\epsilon_1^3\epsilon_2^3}{720} \\ &+ (10\times 4 - 4\times 2 - 4\times 32)\times\frac{6\epsilon_1\epsilon_2^5}{720}\Bigg] \\ = -\frac{1}{180}&(6\epsilon_1^4 + 5\epsilon_1^2\epsilon_2^2 + 6\epsilon_2^4). \end{aligned} \tag{83}$$

Analogously in the x_1x_3 and x_2x_3 planes,

$$\Delta_{j\neq k} = -\frac{1}{180}(6\epsilon_j^4 + 5\epsilon_j^2\epsilon_k^2 + 6\epsilon_k^4). \tag{84}$$

6.6. Partial Scheme, 2-D, 16-point, 4th Order (Fig. 6)

This scheme for the mixed second derivatives is equivalent to the double application of the partial 1-D 5-point scheme (61) for the first derivatives.

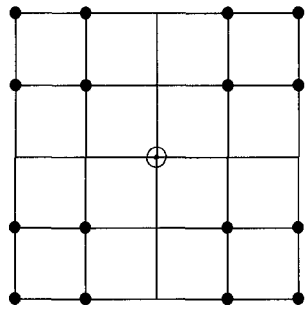

Figure 6

Wave-field grid values (arguments):

$$u_{i(\pm 1,\pm 1,0)},\ u_{i(\pm 2,\pm 1,0)},\ u_{i(\pm 1,\pm 2,0)},\ u_{i(\pm 2,\pm 2,0)}. \tag{85}$$

Determined Taylor-expansion coefficients in addition to 1-D 5-point partial schemes:

$$\begin{gathered} U_{i[12]},\ U_{i[112]},\ U_{i[122]},\ U_{i[1112]},\ U_{i[1122]},\ U_{i[1222]},\ U_{i[11112]},\ U_{i[11122]},\ U_{i[11222]},\ U_{i[12222]}, \\ U_{i[111122]},\ U_{i[111222]},\ U_{i[112222]},\ U_{i[1111222]},\ U_{i[1112222]},\ U_{i[11112222]}. \end{gathered} \tag{86}$$

Most important neglected Taylor-expansion coefficients in addition to 1-D 5-point partial schemes:

$$U_{i[111112]},\ U_{i[122222]},\ U_{i[1111112]},\ U_{i[1111122]},\ U_{i[1122222]},\ U_{i[1222222]}. \tag{87}$$

Finite-difference equation for the second partial derivative inside a geological block:

$$\begin{aligned} 18h^2U_{i12} = 9h^2U_{i[12]} = 8(&u_{i(+1,+1,0)} - u_{i(-1,+1,0)} - u_{i(+1,-1,0)} + u_{i(-1,-1,0)}) \\ &- (u_{i(+2,+1,0)} - u_{i(-2,+1,0)} - u_{i(+2,-1,0)} + u_{i(-2,-1,0)}) \\ &- (u_{i(+1,+2,0)} - u_{i(-1,+2,0)} - u_{i(+1,-2,0)} + u_{i(-1,-2,0)}) \\ &+ \tfrac{1}{8}(u_{i(+2,+2,0)} - u_{i(-2,+2,0)} - u_{i(+2,-2,0)} + u_{i(-2,-2,0)}). \end{aligned} \tag{88}$$

This could take 17 floating-point operations per $18h^2U_{i12}$. However, if the first derivatives resulting from (61) are stored, the evaluation of (88) by means of the second application of (61) takes only *4 additional floating-point operations* per $144h^2U_{i12}$. Relative error in $h^2U_{i[12]} \simeq 2U_i\epsilon_1\epsilon_2$ due to neglecting $h^6U_{i[111112]} \simeq 6U_i\epsilon_1^5\epsilon_2$, and $h^6U_{i[122222]} \simeq 6U_i\epsilon_1\epsilon_2^5$ inside geological blocks:

$$\Delta_{12} = \frac{1}{9}\frac{1}{2\epsilon_1\epsilon_2}\left[\left(8\times 4 - 4\times 32 - 4\times 2 + \frac{1}{8}\times 4\times 64\right)\times\frac{6\epsilon_1^5\epsilon_2}{720}\right.$$
$$\left.+\left(8\times 4 - 4\times 2 - 4\ \times 32 + \frac{1}{8}\times 4\times 64\right)\times\frac{6\epsilon_1\epsilon_2^5}{720}\right]$$
$$= -\frac{1}{180}(6\epsilon_1^4 + 6\epsilon_2^4). \tag{89}$$

Analogously in the x_1x_3 and x_2x_3 planes,

$$\Delta_{j\neq k} = -\frac{1}{180}(6\epsilon_j^4 + 6\epsilon_k^4), \tag{90}$$

which, of course, corresponds to errors (65) of the double application of (61) in directions j and k.

6.7. *Partial Scheme, 1-D, Half-interval 2-point, 2nd Order (Fig. 7)*

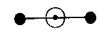

Figure 7

Wave-field grid values (arguments):

$$u_{i(n_1,0,0)},\quad n_1 = -\tfrac{1}{2},\ +\tfrac{1}{2}. \tag{91}$$

Determined Taylor-expansion coefficients:

$$U_i,\ U_{i[1]}. \tag{92}$$

Most important neglected Taylor-expansion coefficients:

$$U_{i[11]},\ U_{i[111]}. \tag{93}$$

Finite-difference equation for the first partial derivative inside a geological block (*1 floating operation* per $hU_{i[1]}$):

$$hU_{i[1]} = u_{i(+\frac{1}{2},0,0)} - u_{i(-\frac{1}{2},0,0)}. \tag{94}$$

This half-interval partial scheme is, as a rule, used to compose second-order staggered schemes. There is no reason to evaluate the half-interval second partial derivative here. Relative error in $hU_{i[1]} \simeq U_i\epsilon_1$ due to neglecting $h^3U_{i[111]} \simeq U_i\epsilon_1^3$ inside geological blocks is

$$\Delta_1 = \frac{1}{\epsilon_1}\left[\frac{1}{8} + \frac{1}{8}\right]\frac{\epsilon_1^3}{6} = \frac{1}{24}\epsilon_1^2. \tag{95}$$

Analogously in the directions of the 2nd and 3rd coordinate axes,

$$\Delta_j = \frac{1}{24}\epsilon_j^2. \tag{96}$$

6.8. Partial Scheme, 1-D, Half-interval 4-point, 4th Order (Fig. 8)

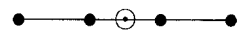

Figure 8

Wave-field grid values (arguments):

$$u_{i(n_1,0,0)}, \quad n_1 = -\tfrac{3}{2}, -\tfrac{1}{2}, +\tfrac{1}{2}, +\tfrac{3}{2}. \tag{97}$$

Determined Taylor-expansion coefficients:

$$U_i, U_{i[1]}, U_{i[11]}, U_{i[111]}. \tag{98}$$

Most important neglected Taylor-expansion coefficients:

$$U_{i[1111]}, U_{i[11111]}. \tag{99}$$

Finite-difference equation for the first partial derivative inside a geological block (*4 floating-point operations* per $24hU_{i[1]}$):

$$24hU_{i[1]} = 27(u_{i(+\frac{1}{2},0,0)} - u_{i(-\frac{1}{2},0,0)}) - (u_{i(+\frac{3}{2},0,0)} - u_{i(-\frac{3}{2},0,0)}). \tag{100}$$

This half-interval partial scheme is, as a rule, used to compose fourth-order staggered schemes. There is no reason to evaluate the half-interval second partial derivative here. Relative error in $hU_{i[1]} \simeq U_i\epsilon_1$ due to neglecting $h^5U_{i[11111]} \simeq U_i\epsilon_1^5$ inside geological blocks is

$$\Delta_1 = \frac{1}{24}\frac{1}{\epsilon_1}\left[27\left(\frac{1}{32}+\frac{1}{32}\right)-\left(\frac{243}{32}+\frac{243}{32}\right)\right]\frac{\epsilon_1^5}{120} = -\frac{3}{640}\epsilon_1^4. \tag{101}$$

Analogously in the directions of the 2nd and 3rd coordinate axes,

$$\Delta_j = -\frac{3}{640}\epsilon_j^4. \tag{102}$$

7. Error Due to the Inaccurate Second Partial Wave-field Derivatives

In this section, we shall study the relative phase-velocity errors of the most important 2-D and 3-D finite-difference schemes on regular rectangular grids in smooth isotropic media.

The relative error of the phase velocity v of the wave of a particular polarization (P, S_1, or S_2), caused by the inaccurate second partial wave-field derivatives, is given by (46) and is real-valued.

In an isotropic medium, see (9), equation (46) reads

$$\Delta^{(1)} \simeq \frac{1}{2} \frac{\sum_{j,k} [(\lambda + \mu) e_j e_k + \mu \delta_{jk}] \epsilon_j \epsilon_k \Delta_{jk}}{\rho v^2 \epsilon^2}$$

$$= \frac{1}{2} \frac{\sum_{j,k} [(v_P^2 - v_S^2) e_j e_k + v_S^2 \delta_{jk}] \epsilon_j \epsilon_k \Delta_{jk}}{v^2 \epsilon^2}$$

$$= \frac{1}{2v^2} \left\{ \sum_j [(v_P^2 - v_S^2) e_j^2 + v_S^2] \epsilon_j^2 \Delta_{jj} + 2 \sum_{j<k} (v_P^2 - v_S^2) e_j e_k \epsilon_j \epsilon_k \Delta_{jk} \right\} \epsilon^{-2}. \tag{103}$$

In a special case of the propagation along a gridline, relative phase-velocity error (103) of the elastic waves is the same as the error of the acoustic waves,

$$\Delta^{(1)}_{\text{gridline}} = \tfrac{1}{2} \Delta_{jj} \tag{104}$$

with ϵ substituted for ϵ_j in Δ_{jj}.

Note that if $\Delta_{jk} = \Delta_j + \Delta_k$ (e.g., for staggered grids or the methods based on the first-order systems of equations for u_i and stress σ_{ij}), equation (103) simplifies to

$$\Delta^{(1)} \simeq \left\{ \sum_j \epsilon_j^2 \Delta_j \right\} \epsilon^{-2} \tag{105}$$

independently of the wave polarization, as already noticed by VIRIEUX (1986). If partial relative error Δ_j has its maximum along the gridlines in the jth direction, then the maximum relative phase-velocity error is incurred along the gridlines,

$$\Delta^{(1)}_{\max} = \Delta_j \tag{106}$$

with ϵ substituted for ϵ_j in Δ_j.

Now the relative errors corresponding to the particular finite-difference schemes must be substituted for Δ_{jk} into (103) to arrive at the final error estimates.

7.1. 2-D, 9-point, 2nd Order (Fig. 9)

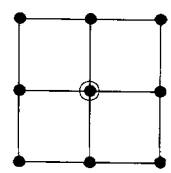

Figure 9

This scheme, used for elastic waves in cylindrical coordinates by ALTERMAN and KARAL (1968), is composed of 1-D 3-point and 2-D 4-point partial schemes,

and requires *10 floating-point operations × 2 components* per $2hU_{I1}$, $2hU_{I2}$, h^2U_{I11}, h^2U_{I22}, h^2U_{I12}. Equation (103) with (57) and (72) reads

$$\Delta^{(1)} \simeq \frac{1}{24v^2}\left\{\sum_j [(v_P^2 - v_S^2)e_j^2 + v_S^2]\epsilon_j^4 + 4\sum_{j<k}(v_P^2 - v_S^2)e_j e_k(\epsilon_j^3\epsilon_k + \epsilon_j\epsilon_k^3)\right\}\epsilon^{-2}. \quad (107)$$

Unfortunately, this equation does not conform with the grid dispersion curves shown by MARFURT (1984). On the other hand, for propagation along the gridline, it conforms with the grid dispersion relation for acoustic waves derived by ALFORD *et al.* (1974), see also equation (10) by DABLAIN (1986).

The maximum relative P-wave phase-velocity error for $v_P^2 \leq 3v_S^2$ is incurred along the gridlines,

$$\Delta_{\max}^{(1)} = \frac{1}{24}\epsilon^2. \quad (108)$$

The maximum relative P-wave phase-velocity error for $v_P^2 \geq 3v_S^2$ is greater and is incurred along the diagonals,

$$\Delta_{\max}^{(1)} = \frac{1}{24}\left(\frac{5}{4} - \frac{3}{4}\frac{v_S^2}{v_P^2}\right)\epsilon^2. \quad (109)$$

The maximum relative S-wave phase-velocity error for $v_P^2 \leq 3v_S^2$ is incurred along the gridlines,

$$\Delta_{\max}^{(1)} = \frac{1}{24}\epsilon^2. \quad (110)$$

The maximum relative S-wave phase-velocity error for $v_P^2 \geq 3v_S^2$ is greater and is incurred for the in-plane polarization propagating along the diagonals,

$$\Delta_{\max}^{(1)} = -\frac{1}{24}\left(\frac{3}{4}\frac{v_P^2}{4v_S^2} - \frac{5}{4}\right)\epsilon^2. \quad (111)$$

7.2. 2-D, 17-point, 4th Order (Fig. 10)

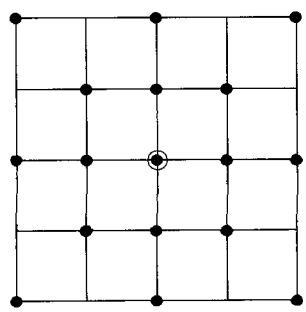

Figure 10

This scheme is composed of 1-D 5-point and 2-D 8-point partial schemes, and requires *29 floating-point operations × 2 components* per $12hU_{I1}$, $12hU_{I2}$, $12h^2U_{I11}$, $12h^2U_{I22}$, $12h^2U_{I12}$. Equation (103) with (66) and (78) reads

$$\Delta^{(1)} \simeq -\frac{1}{180v^2}\left\{\sum_j [(v_P^2 - v_S^2)e_j^2 + v_S^2]\epsilon_j^6 + \sum_{j<k} (v_P^2 - v_S^2)e_j e_k(6\epsilon_j^5\epsilon_k + 20\epsilon_j^3\epsilon_k^3 + 6\epsilon_j\epsilon_k^5)\right\}\epsilon^{-2}. \tag{112}$$

The maximum relative P-wave phase-velocity error is incurred along the diagonals,

$$\Delta_{\max}^{(1)} = -\frac{1}{180}\left(\frac{17}{8} - \frac{15}{8}\frac{v_S^2}{v_P^2}\right)\epsilon^4. \tag{113}$$

For example, the value of (113) for $v_P^2 = 3v_S^2$ is

$$\Delta_{\max}^{(1)} = -\frac{1}{180}\frac{3}{2}\epsilon^4. \tag{114}$$

The maximum relative S-wave phase-velocity error is incurred for the in-plane polarization propagating along the diagonals,

$$\Delta_{\max}^{(1)} = \frac{1}{180}\left(\frac{15}{8}\frac{v_P^2}{v_S^2} - \frac{17}{8}\right)\epsilon^4. \tag{115}$$

For example, the value of (115) for $v_P^2 = 3v_S^2$ is

$$\Delta_{\max}^{(1)} = \frac{1}{180}\frac{7}{2}\epsilon^4. \tag{116}$$

7.3. 2-D, 21-point, 4th Order (Fig. 11)

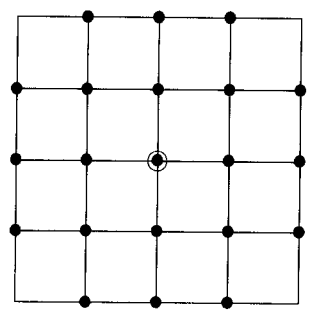

Figure 11

This scheme is composed of 1-D 5-point and 2-D 12-point partial schemes, and requires *33 floating-point operations × 2 components* per $12hU_{I1}$, $12hU_{I2}$, $12h^2U_{I11}$, $12h^2U_{I22}$, $12h^2U_{I12}$. Equation (103) with (66) and (84) reads

$$\Delta^{(1)} \simeq -\frac{1}{180v^2}\left\{\sum_j [(v_P^2 - v_S^2)e_j^2 + v_S^2]\epsilon_j^6 + \sum_{j<k} (v_P^2 - v_S^2)e_j e_k (6\epsilon_j^5\epsilon_k + 5\epsilon_j^3\epsilon_k^3 + 6\epsilon_j\epsilon_k^5)\right\}\epsilon^{-2}. \tag{117}$$

The maximum relative P-wave phase-velocity error for $v_P^2 \leq \frac{5}{2}v_S^2$ is incurred along the gridlines,

$$\Delta_{\max}^{(1)} = -\frac{1}{180}\epsilon^4. \tag{118}$$

The maximum relative P-wave phase-velocity error for $v_P^2 > \frac{5}{2}v_S^2$ is greater and is incurred in the direction of unit vector $(\vartheta_1, \vartheta_2) = (\cos\alpha, \sin\alpha)$ satisfying equation

$$(\cos\alpha)^2(\sin\alpha)^2 = \frac{1}{5}\frac{v_P^2 - \frac{5}{2}v_S^2}{v_P^2 - v_S^2}, \tag{119}$$

and is equal to

$$\Delta_{\max}^{(1)} = -\frac{1}{180}\left[1 + \frac{1}{5}\frac{(v_P^2 - \frac{5}{2}v_S^2)^2}{v_P^2(v_P^2 - v_S^2)}\right]\epsilon^4. \tag{120}$$

For example, the value of (120) for $v_P^2 = 3v_S^2$ is

$$\Delta_{\max}^{(1)} = -\frac{1}{180}\frac{121}{120}\epsilon^4. \tag{121}$$

The maximum relative S-wave phase-velocity error for $v_P^2 \leq \frac{7}{3}v_S^2$ is incurred along the gridlines,

$$\Delta_{\max}^{(1)} = -\frac{1}{180}\epsilon^4. \tag{122}$$

The maximum relative S-wave phase-velocity error for $v_P^2 > \frac{7}{3}v_S^2$ is greater and is incurred for the in-plane polarization propagating along the diagonals,

$$\Delta_{\max}^{(1)} = \frac{1}{180}\left(\frac{15}{16}\frac{v_P^2}{v_S^2} - \frac{19}{16}\right)\epsilon^4. \tag{123}$$

For example, the value of (123) for $v_P^2 = 3v_S^2$ is

$$\Delta_{\max}^{(1)} = \frac{1}{180}\frac{13}{8}\epsilon^4. \tag{124}$$

7.4. 2-D, 25-point, 4th Order (Fig. 12)

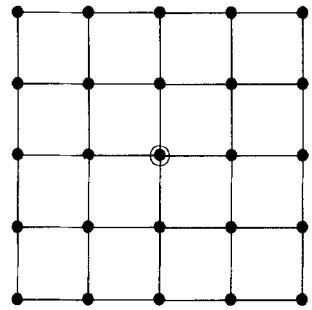

Figure 12

This scheme is composed of 1-D 5-point and 2-D 16-point partial schemes, and requires *25 floating-point operations × 2 components* per $12hU_{I1}$, $12hU_{I2}$, $12h^2U_{I11}$, $12h^2U_{I22}$, $12h^2U_{I12}$. Equation (103) with (66) and (90) reads

$$\Delta^{(1)} \simeq -\frac{1}{180v^2}\left\{\sum_j [(v_P^2 - v_S^2)e_j^2 + v_S^2]\epsilon_j^6 + \sum_{j<k} (v_P^2 - v_S^2)e_j e_k(6\epsilon_j^5\epsilon_k + 6\epsilon_j\epsilon_k^5)\right\}\epsilon^{-2}. \tag{125}$$

For the propagation along a gridline, equations (112), (117) and (125) give, naturally, the same relative phase-velocity error, conformal with the grid dispersion relation for acoustic waves published by ALFORD *et al.* (1974).

The maximum relative P-wave phase-velocity error for $v_P^2 \leq \frac{5}{2}v_S^2$ is incurred along the gridlines,

$$\Delta^{(1)}_{\max} = -\frac{1}{180}\epsilon^4. \tag{126}$$

The maximum relative P-wave phase-velocity error for $v_P^2 > \frac{5}{2}v_S^2$ is greater and is incurred in the direction of unit vector $(\vartheta_1, \vartheta_2) = (\cos\alpha, \sin\alpha)$ satisfying equation

$$(\cos\alpha)^2(\sin\alpha)^2 = \frac{1}{10}\frac{v_P^2 - \frac{5}{2}v_S^2}{v_P^2 - v_S^2}, \tag{127}$$

and is equal to

$$\Delta^{(1)}_{\max} = -\frac{1}{180}\left[1 + \frac{1}{10}\frac{(v_P^2 - \frac{5}{2}v_S^2)^2}{v_P^2(v_P^2 - v_S^2)}\right]\epsilon^4. \tag{128}$$

For example, the value of (128) for $v_P^2 = 3v_S^2$ is

$$\Delta^{(1)}_{\max} = -\frac{1}{180}\frac{241}{240}\epsilon^4. \tag{129}$$

The maximum relative S-wave phase-velocity error for $v_P^2 \leq 3v_S^2$ is incurred along the gridlines,

$$\Delta_{\max}^{(1)} = -\frac{1}{180}\epsilon^4. \tag{130}$$

The maximum relative S-wave phase-velocity error for $v_P^2 > 3v_S^2$ is greater and is incurred for the in-plane polarization propagating along the diagonals,

$$\Delta_{\max}^{(1)} = \frac{1}{180}\left(\frac{5}{8}\frac{v_P^2}{v_S^2} - \frac{7}{8}\right)\epsilon^4. \tag{131}$$

Thus, in an isotropic medium, this scheme is both computationally faster and more accurate, for both P waves and S waves, than the preceding 17-point and 21-point schemes. The disadvantage of this scheme is that the first wave-field derivatives must be evaluated two grid intervals ahead and kept in the memory in order to retain the computational speed.

7.5. 3-D, 19-point, 2nd Order (Fig. 13)

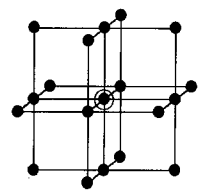

Figure 13

This scheme is composed of 1-D 3-point and 2-D 4-point partial schemes. In view of (14) we see that not all 3 mixed second derivatives of all 3 wave-field components are needed. It is sufficient to calculate only

$$\frac{\partial}{\partial x^1}(u_{2,2} + u_{3,3}), \quad \frac{\partial}{\partial x^2}(u_{1,1} + u_{3,3}), \quad \frac{\partial}{\partial x^3}(u_{1,1} + u_{2,2}) \tag{132}$$

by means of the second application of (52). Costs may thus be reduced even to *15 floating-point operations × 3 components* per $2hU_{i1}$, $2hU_{i2}$, $2hU_{i3}$, h^2U_{i11}, h^2U_{i22}, h^2U_{i33}, $h^2\,\Sigma_{j\neq i}\,U_{jji}$.

The accuracy is identical to the *2-D, 9-point, 2nd order* scheme, see (107) to (111).

7.6. 3-D, 37-point, 4th Order (Fig. 14)

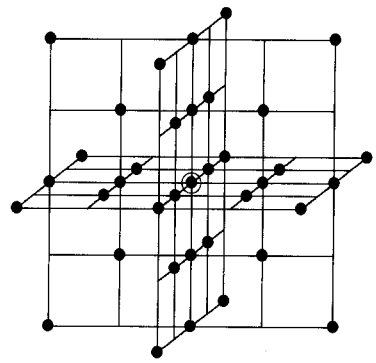

Figure 14

This scheme is composed of 1-D 5-point and 2-D 8-point partial schemes, and requires *48 floating-point operations × 3 components.*

The accuracy is identical to the *2-D, 17-point, 4th order* scheme, see (112) to (116).

7.7. 3-D, 49-point, 4th Order (Fig. 15)

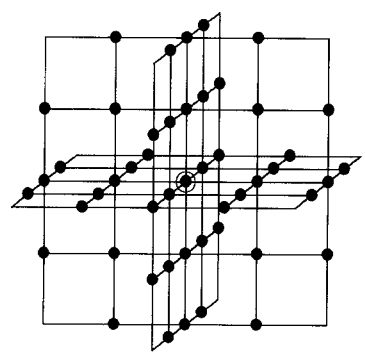

Figure 15

This scheme is composed of 1-D 5-point and 2-D 12-point partial schemes, and requires *56 floating-point operations × 3 components* per $12hU_{i1}$, $12hU_{i2}$, $12hU_{i3}$, $12h^2U_{i11}$, $12h^2U_{i22}$, $12h^2U_{i33}$, $12h^2\,\Sigma_{j\neq i}\,U_{jji}$.

The accuracy is identical to the *2-D, 21-point, 4th order* scheme, see (117) to (124).

7.8. 3-D, 61-point, 4th Order (Fig. 16)

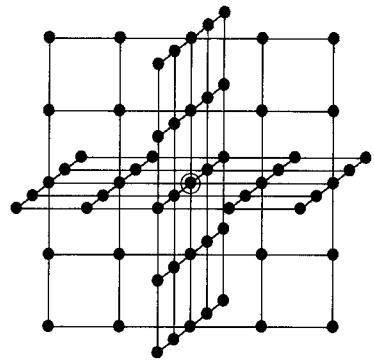

Figure 16

This scheme is composed of 1-D 5-point and 2-D 16-point partial schemes. In view of (14) we see that not all 3 mixed second derivatives of all 3 wave-field components are needed. It is sufficient to calculate only

$$\frac{\partial}{\partial x^1}(u_{2,2}+u_{3,3}),\quad \frac{\partial}{\partial x^2}(u_{3,3}+u_{1,1}),\quad \frac{\partial}{\partial x^3}(u_{1,1}+u_{2,2}) \tag{133}$$

by means of the second application of (61). Costs may thus be reduced even to *36 floating-point operations × 3 components* per $12hU_{i1}$, $12hU_{i2}$, $12hU_{i3}$, $12h^2U_{i11}$, $12h^2U_{i22}$, $12h^2U_{i33}$, $12h^2\,\Sigma_{j\neq i}\,U_{jji}$, provided that $U_{22}+U_{33}$, $U_{33}+U_{11}$ and $U_{11}+U_{22}$ at surrounding gridpoints are temporarily stored in the memory.

The accuracy is identical to the *2-D, 25-point, 4th order* scheme, see (125) to (131).

7.9. Staggered Finite-difference Schemes

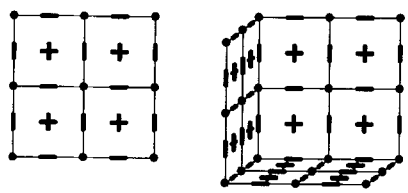

Figure 17

The staggered schemes according to MADARIAGA (1976), VIRIEUX and MADARIAGA (1982), VIRIEUX (1986), and LEVANDER (1988) are composed of 1-D half-interval partial schemes. Since accuracy of the double application of first finite differences of the 2nd order in time, once for the stress and once for the wave field, is equal to the accuracy of the second finite differences (36), we will follow IGEL

et al. (1991) and SEI (1993) in using equations (8) and (11) at a time instant and equation (36) with respect to time.

The components of the wave-field vector are discretized half way between gridpoints along the corresponding gridlines, their partial derivatives U_{ij} and stress components σ_{ij} for $i=j$ at the gridpoints, and for $i \neq j$ at the centers of the square faces formed by gridlines parallel with the ith and jth axes (Fig. 17). Material parameters are assumed to be specified at gridpoints (i.e., intersections of the gridlines), linearly interpolated along gridline intervals, and bilinearly interpolated within the square faces.

Inserting (9) into (8) we arrive at

$$\sigma_{i=j}(\mathbf{x}) = 2\mu(\mathbf{x})u_{i,j}(\mathbf{x}) + \lambda(\mathbf{x}) \sum_k u_{k,k}(\mathbf{x}) \tag{134}$$

and

$$\sigma_{i\neq j}(\mathbf{x}) = [u_{i,j}(\mathbf{x}) + u_{j,i}(\mathbf{x})] \frac{1}{8} \sum_{\pm\pm} 2\mu(\mathbf{x} \pm \tfrac{1}{2}\mathbf{h}_i \pm \tfrac{1}{2}\mathbf{h}_j). \tag{135}$$

Here $2\mu(\mathbf{x})$ in the center of the square face has been replaced by its bilinear approximation from the corner gridpoints of the face. Using linear interpolation of the density between the gridpoints, equation (11) reads

$$u_i''(\mathbf{x}) = \frac{2\sum_j \sigma_{ij,j}(\mathbf{x})}{\rho(\mathbf{x} - \tfrac{1}{2}\mathbf{h}_i) + \rho(\mathbf{x} + \tfrac{1}{2}\mathbf{h}_i)}. \tag{136}$$

These equations, together with (36) and the 1-D half-interval partial schemes of the corresponding order, define the staggered finite-difference method considered here.

7.10. 2-D Staggered, 2nd Order (Fig. 18)

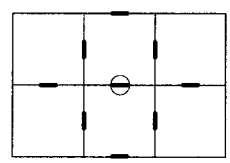

Figure 18

This scheme is composed of 1-D 2-point half-interval partial schemes of Section 6.7. Equation (105) with (96) reads

$$\Delta^{(1)} \simeq \frac{1}{24\epsilon^2} \sum_j \epsilon_j^4. \tag{137}$$

This equation conforms with grid dispersion curves shown by VIRIEUX (1986).

The maximum relative phase-velocity error is incurred along the gridlines,

$$\Delta^{(1)}_{\max} = \frac{1}{24}\epsilon^2, \tag{138}$$

see (106) with (96), and is dependent on the wave polarization through ϵ only.

7.11. 2-D Staggered, 4th Order (Fig. 19)

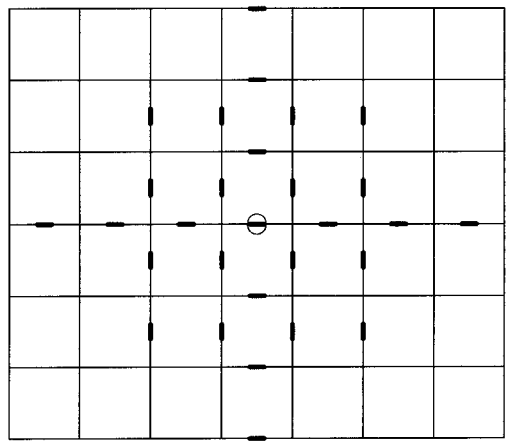

Figure 19

This scheme is composed of 1-D 4-point half-interval partial schemes of Section 6.8. Equation (105) with (102) reads

$$\Delta^{(1)} \simeq -\frac{3}{640\epsilon^2}\sum_j \epsilon_j^6. \tag{139}$$

The maximum relative phase-velocity error is incurred along the gridlines,

$$\Delta^{(1)}_{\max} = -\frac{3}{640}\epsilon^4, \tag{140}$$

see (106) with (96), and is dependent on the wave polarization through ϵ only.

This staggered 4th order finite-difference scheme is thus slightly more accurate than the centered 25 point 2-D 4th order finite-difference scheme of Section 7.4, but has an extent of 6 grid intervals that would correspond to the centered finite-difference scheme of the 6th order.

7.12. 3-D Staggered, 2nd Order (Fig. 20)

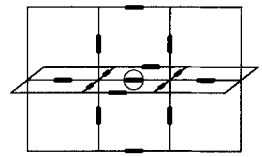

Figure 20

This scheme is composed of 1-D 2-point half-interval partial schemes of Section 6.7.

The accuracy is identical to the 2-D staggered 2nd order scheme, see (137) and (138).

7.13. 3-D Staggered, 4th Order (Fig. 21)

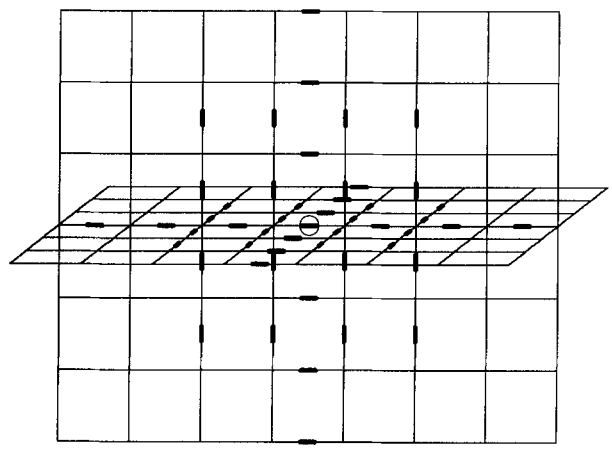

Figure 21

This scheme is composed of 1-D 4-point half-interval partial schemes of Section 6.8.

The accuracy is identical to the 2-D staggered 4th order scheme, see (139) and (140).

8. Error Due to the Inaccurate Wave-field Gradient

Inserting (56) into (47), we arrive at the estimate

$$\Delta^{(2)} \simeq \frac{1}{12} \frac{h}{\rho v^2 \epsilon^2} e_i e_k \sum_{l=1}^{3} C_{ijkl} (\epsilon_l)^3 \tag{141}$$

of the relative phase-velocity error due to the approximation of the wave-field gradient by finite differences of the second order. Similarly, inserting (65) into (47), we arrive at the estimate

$$\Delta^{(2)} \simeq -\frac{1}{60}\frac{h}{\rho v^2 \epsilon^2} e_i e_k \sum_{l=1}^{3} C_{ijkl} (\epsilon_l)^5 \tag{142}$$

of the relative phase-velocity error due to the approximation of the wave-field gradient by finite differences of the fourth order.

In an isotropic medium, the relative phase-velocity error is thus

$$\Delta^{(2)} \simeq \frac{1}{12}\frac{h}{\rho v^2 \epsilon^2} \sum_{l=1}^{3} \frac{\partial(\rho v^2)}{\partial x_l} (\epsilon_l)^3 \tag{143}$$

for the finite differences of the 2nd order, and

$$\Delta^{(2)} \simeq -\frac{1}{60}\frac{h}{\rho v^2 \epsilon^2} \sum_{l=1}^{3} \frac{\partial(\rho v^2)}{\partial x_l} (\epsilon_l)^5 \tag{144}$$

for the finite differences of the 4th order. Relative errors (143) and (144) are independent of the wave polarization.

If we denote, in an isotropic medium,

$$\frac{1}{L^{(1)}} = \max\left(\left| \frac{1}{\rho v^2} \frac{\partial(\rho v^2)}{\partial x_j} \right|, j = 1, 2, 3 \right), \tag{145}$$

the maximum absolute value of the imaginary relative phase-velocity error due to the inaccurate wave-field gradient is

$$\Delta^{(2)}_{\max} \simeq \frac{|\epsilon|}{12}\frac{h}{L^{(1)}} \tag{146}$$

for the finite differences of the 2nd order, and

$$\Delta^{(2)}_{\max} \simeq \frac{|\epsilon|^3}{60}\frac{h}{L^{(1)}} \tag{147}$$

for the finite differences of the 4th order. This maximum error is incurred if the wave propagates along the corresponding gridline, and should be negligible in reasonably sampled models.

Equations (141), (143) and (146) for the 2nd order centered finite differences are applicable also to the 2nd order staggered finite differences. Equations (142), (144) and (147) are in force only for the 4th order centered finite differences, still similar expressions for the 4th order staggered finite differences can be derived.

9. Error Due to the Inaccurate Gradients of Material Parameters

The error of approximation (17) is

$$\delta(C_{ijklm}) \simeq \frac{h^2}{6} \frac{\partial^3 c_{ijkl}}{(\partial x_m)^3}(\mathbf{x}). \tag{148}$$

Inserting (148) into (48) we arrive at

$$\Delta^{(3)} \simeq \frac{1}{12} \frac{h^3}{\rho v^2 \epsilon^2} e_i e_k \epsilon_l \sum_{j=1}^{3} \frac{\partial^3 c_{ijkl}}{(\partial x_j)^3}(\mathbf{x}). \tag{149}$$

In an isotropic medium, the relative phase-velocity error is thus

$$\Delta^{(3)} \simeq \frac{1}{12} \frac{h^3}{\rho v^2 \epsilon^2} \sum_{j=1}^{3} \epsilon_j \frac{\partial^2(\rho v^2)}{(\partial x_j)^3}. \tag{150}$$

Relative error (150) is independent of the wave polarization.

If we denote, in an isotropic medium,

$$\frac{1}{L^{(3)}} = \max\left(\left|\frac{1}{\rho v^2} \frac{\partial^3(\rho v^2)}{(\partial x_j)^3}\right|, j = 1, 2, 3\right), \tag{151}$$

the maximum absolute value of the imaginary relative phase-velocity error due to the inaccurate gradient of the elastic parameters is

$$\Delta^{(3)}_{\max} \simeq \frac{1}{12|\epsilon|} \frac{h^3}{L^{(3)}}. \tag{152}$$

Here ϵ in the denominator looks dangerously for low frequencies at first glance, but implies no problems. Relative phase-velocity error (152) causes an error of the order of $\frac{1}{12} h^2/L^{(2)}$, with

$$\frac{1}{L^{(2)}} = \max\left(\left|\frac{1}{\rho v^2} \frac{\partial^2(\rho v^2)}{(\partial x_j)^2}\right|, j = 1, 2, 3\right), \tag{153}$$

in the wave-field amplitudes, independently of the wavelength. Such an error should be negligible in all reasonably sampled models, independently of the order of the finite-difference scheme used.

This error is 4 times reduced for staggered finite differences of the 2nd order, and is even much smaller for staggered finite differences of the 4th order.

10. Error Due to the Inaccurate Values of Material Parameters

Staggered finite differences introduce another, usually also negligible, real-valued relative phase-velocity error due to the interpolation of the material parameters between the gridpoints. The bilinear and linear interpolations are explicitly ex-

pressed in equation (135) and in the denominator of equation (136), however the linear interpolation of material parameters between gridpoints, hidden in the numerator of (136), also takes place if staggered finite differences of the 2nd order are used.

For example, maximum absolute relative phase-velocity error due to the inaccurate values of material parameters, corresponding to a wave propagating along a gridline, is

(a) for P wave calculated by staggered finite differences of the 2nd order

$$\Delta^{(4)}_{\max} \simeq \frac{1}{16}\frac{h^2}{\Lambda^{(2)}}, \tag{154}$$

(b) for S wave calculated by staggered finite differences of the 2nd order

$$\Delta^{(4)}_{\max} \lesssim \frac{1}{16}\frac{h^2}{\Lambda^{(2)}} + \frac{1}{8}\frac{h^2}{L^{(2)}}, \tag{155}$$

(c) for P wave calculated by staggered finite differences of the 4th order

$$\Delta^{(4)}_{\max} \simeq \frac{1}{16}\frac{h^2}{R^{(2)}}, \tag{156}$$

(d) for S wave calculated by staggered finite differences of the 4th order

$$\Delta^{(4)}_{\max} \lesssim \frac{1}{16}\frac{h^2}{\Lambda^{(2)}} + \frac{1}{16}\frac{h^2}{L^{(2)}}, \tag{157}$$

with

$$\frac{1}{\Lambda^{(2)}} = \max\left(\left|\frac{1}{v^2}\frac{\partial^2(v^2)}{(\partial x_j)^2}\right|, j = 1, 2, 3\right) \tag{158}$$

and

$$\frac{1}{R^{(2)}} = \max\left(\left|\frac{1}{\rho}\frac{\partial^2 \rho}{(\partial x_j)^2}\right|, j = 1, 2, 3\right). \tag{159}$$

The maximum absolute relative phase-velocity errors in other directions will likely not differ considerably from these estimates.

11. Efficiency Estimations

11.1. Centered Point 2-D and 3-D Schemes

Assume the use of the best 4th order schemes of Sections 7.4 or 7.8, and to have also stored, in addition to the wave-field components in 2 times instants, isotropic elastic parameters λ, μ and $(12h^2/H^2)\rho$ in the computer RAM (random-access memory).

Evaluation of $12h^2U_{i1}$, $12h^2U_{i2}$, $12h^2U_{i3}$ (in 3-D), $12h^2U_{i11}$, $12h^2U_{i22}$, $12h^2U_{i33}$ (in 3-D), $12h^2\,\Sigma_{j\neq i}\,U_{jji}$ using the 4th order schemes of Sections 7.4 or 7.8 requires *25 (in 2-D)* or *36 (in 3-D) floating-point operations per component*. For this class of even-order finite-difference schemes, the number of floating-point operations per component increases by 15 (in 2-D) or 21 (in 3-D) if the order of the scheme is increased by 2.

Evaluation of $2h(\partial\lambda/\partial x_i)(\mathbf{x})$, $2h(\partial\mu/\partial x_i)(\mathbf{x})$ using (17) requires *2 additional floating-point operations per component*.

Evaluation of $12h^2C_{ijklj}U_{kl}$ using (16) requires *8 (in 2-D)* or *10 + 2/3 (in 3-D) additional floating-point operations per component*.

Evaluation of $12h^2C_{ijkl}U_{klj}$ using (14) requires *5 (in 2-D)* or *6 (in 3-D) additional floating-point operations per component*, plus *1 floating-point operation* for the addition in $\lambda + \mu$.

Evaluation of $H^2u_i''(\mathbf{x})$ using (12) requires *2 additional floating-point operations per component*.

Finally, evaluation of (36) requires *3 additional floating-point operations per component*.

The total number of floating-point operations per gridpoint, required to calculate the elastic wave field in the next time instant using the finite-difference scheme of the 4th order, is thus $45 \times 2 + 1 = 91$ *floating-point operations* in 2-D, or $59 \times 3 + 2 + 1 = 180$ *floating-point operations* in 3-D.

In general, the total number of floating-point operations per gridpoint, required to calculate the elastic wave field in the next time instant using the centered finite-difference scheme of the Kth order, is $31 + 30\,K/2$ *floating-point operations* in 2-D, or $54 + 63K/2$ *floating-point operations* in 3-D.

11.2. Staggered 2-D and 3-D Schemes

Assume the use of the staggered schemes of Sections 7.9 to 7.13 and to have stored, in addition to the wave-field components at "staggered" points in 2 time instants, also isotropic elastic parameters λ, 2μ, and $\rho c^2/(2H^2)$ at gridpoints in the computer RAM (random-access memory). Here $c = h$ for the 2nd order scheme (94), and $c = 24h$ for the 4th order scheme (100).

Calculation of $c\sigma_{i=j}$ from $cU_{k=l}$ using (134) requires *3 floating-point operations × 2 or 3 components*.

Calculation of $c\sigma_{i\neq j}$ from cU_{ij} and cU_{ji} using (135) requires *6 floating-point operations* in 2-D and *18 floating-point operations* in 3-D.

Evaluation of $H^2u_i''(\mathbf{x})$ from $c^2\sigma_{ij,j}$ using (136) requires *6 floating-point operations* in 2-D and *12 floating-point operations* in 3-D.

Finally, evaluation of (36) requires *3 additional floating-point operations per component*.

In total, staggered finite differences require *24 floating-point operations* plus evaluation of *8 partial schemes* in 2-D and *48 floating-point operations* plus evaluation of *18 partial schemes* in 3-D.

Evaluation of half-interval 2nd order partial scheme of Section 6.7 costs *1 floating-point operation*, whereas evaluation of half-interval 4th order partial scheme of Section 6.8 costs *4 floating-point operations*. In general, evaluation of half-interval Kth order partial scheme costs $-2+3K/2$ *floating-point operations*.

The total number of floating-point operations per gridpoint, required to calculate the elastic wave field in the next time instant using the staggered finite-difference scheme of the Kth order, is $8+24K/2$ *floating-point operations* in 2-D, or $12+54K/2$ *floating-point operations* in 3-D. For instance, the staggered finite differences of the 4th order require *56 floating-point operations* per gridpoint in 2-D, and *120 floating-point operations* per gridpoint in 3-D.

12. Conclusions

The error analysis discloses that, in smooth parts of the model, the most severe errors are due to the finite-difference approximation of the second space derivatives of the wave field. Such errors cannot be reduced by applying some averaged "effective" material parameters. In this way, the application of purely point schemes inside geological blocks is justified.

For elastic waves in smooth parts of an isotropic medium, the fastest centered 2-D second-order finite-difference scheme is the scheme of Section 7.1, evaluating the mixed second partial wave-field derivatives by double application of the second-order 1-D scheme of Section 6.1. The fastest centered 3-D second-order scheme is its direct 3-D extension shown in Section 7.5.

Staggered second-order finite-difference schemes of Sections 7.10 (2-D) and 7.12 (3-D) are nearly twice faster than the centered second-order schemes, with the same accuracy for both P waves and S waves if $v_P^2 \leq 3v_S^2$, and with much better accuracy for slowly propagating S waves ($v_P^2 \gg 3v_S^2$).

The best (both most accurate and fastest) centered 2-D fourth-order finite-difference scheme is the scheme of Section 7.4, evaluating the mixed second partial wave-field derivatives by double application of the fourth-order 1-D scheme of Section 6.2. The best centered 3-D fourth-order scheme is its direct 3-D extension shown in Section 7.8. The wave field and the elastodynamic parameters are assumed to be differenced independently.

Staggered fourth-order finite-difference schemes of Sections 7.11 (2-D) and 7.13 (3-D) are about 3/2 times faster than the centered fourth-order schemes, with 27/32 times smaller error for both P waves and S waves if $v_P^2 \leq 3v_S^2$, and with considerably better accuracy for slowly propagating S waves ($v_P^2 \gg 3v_S^2$). The disadvantage of staggered fourth-order finite differences is their extent along a gridline, corre-

sponding to the centered sixth-order scheme (in general, the size of the staggered scheme of the Kth order along a gridline is $2K-2$ grid intervals, which corresponds to the centered scheme of the $(2K-2)$th order).

The fourth-order finite-difference schemes are undoubtedly superior to the second-order ones.

The relative phase-velocity error of the wave of a particular polarization and direction of propagation is given by (45), with its individual components derived in Sections 5.1, 7, 8, 9 and 10. In particular, the individual contributions to the relative phase-velocity error for the best centered 2-D and 3-D fourth-order spatial finite-difference schemes for the wave field with the second-order time integration are given by equations (38), (125), (144) and (150), where error (125) due to the inaccurate second partial wave-field derivatives is dominant. This dominant error is given by (107) for the centered second-order finite differences, (125) for the centered fourth-order finite differences, (137) for the staggered second-order finite differences and (139) for the staggered fourth-order finite differences.

Acknowledgements

The author is indebted to Heiner Igel, Ivan Pšenčík, and Jiří Zahradník for their essential comments and assistance during preparation of the final version of the manuscript.

The research was supported by the Grant Agency of the Czech Republic under Contract 205/95/1465, and by the Institute Français du Pétrole, the Shell Research B.V., the Japan National Oil Corporation, and the Elf Geoscience Research Centre within the consortium project "Seismic Waves in Complex 3-D Structures."

REFERENCES

ABRAMOWITZ, M., and STEGUN, I. A., *Handbook of Mathematical Functions* (National Bureau of Standards, Washington, D.C. 1964).

ALFORD, R. M., KELLY, K. R., and BOORE, D. M. (1974), *Accuracy of Fnite-difference Modeling of the Acoustic Wave Equation*, Geophysics *39*, 834–842.

ALTERMAN, Z., and KARAL, F. C. (1968), *Propagation of Elastic Waves in Layered Media by Finite-difference Method*, Bull. Seismol. Soc. Am. *58*, 367–398.

BICKLEY, W. G. (1941), *Formulae for Numerical Differentiation*, Math. Gaz. *25*, 19–27.

DABLAIN, M. A. (1986), *The Application of High-order Differencing to the Scalar Wave Equation*, Geophysics *51*, 54–66.

FORNBERG, B. (1988), *Generation of Finite Difference Formulas on Arbitrary Spaced Grids*, Math. Computation *51*, 699–706.

IGEL, H., MORA, P., and RIOLLET, B. (1995), *Anisotropic Wave Propagation Through Finite-difference Grids*, Geophysics *60*, 1203–1216.

IGEL, H., MORA, P., and RODRIGUES, D. (1991), *3-D Wave Propagation Using Finite Differences*, Expanded Abstracts, 61st Annual Int. SEG Meeting, pp. 1577–1579, Soc. Exploration Geophysicists, Tulsa.

KELLER, H. B., and PEREYRA, V. (1978), *Symbolic Generation of Finite Difference Formulas*, Math. Computation *32*, 955–971.

LEVANDER, A. R. (1988), *Fourth-order Finite-difference P-SV Seismograms*. Geophysics *53*, 1425–1436.

MADARIAGA, R. (1976), *Dynamics of an Expanding Circular Fault*, Bull. Seismol. Soc. Am. *66*, 639–666.

MARFURT, K. J. (1984), *Accuracy of Finite-difference and Finite-element Modeling of the Scalar and Elastic Wave Equations*, Geophysics *49*, 533–549.

SEI, A. (1993), *Computational Cost of Finite-difference Elastic Waves Modeling*, Expanded Abstracts, 63rd Annual Int. SEG Meeting, pp. 1065–1068, Soc. Exploration Geophysicists, Tulsa.

STEPHEN, R. A. (1988), *A Review of Finite Difference Methods for Seismo-acoustics Problems at the Seafloor*, Rev. Geophys. *26*, 445–458.

VIRIEUX, J., and MADARIAGA, R. (1982), *Dynamic Faulting Studied by a Finite Difference Method*, Bull. Seismol. Soc. Am. *72*, 345–369.

VIRIEUX, J. (1986), *P-SV Wave Propagation in Heterogeneous Media: Velocity-stress Finite-difference Method*, Geophysics *51*, 889–901.

(Received August 14, 1995, revised/accepted March 27, 1996)